Available online at www.sciencedirect.com
SCIENCE DIRECT
International Journal of Heat and Fluid Flow 27 (2006) 661–670
International Journal of HEAT AND FLUID FLOW
www.elsevier.com/locate/ijhff

Numerical prediction of shock induced oscillations over a 2D airfoil: Influence of turbulence modelling and test section walls

Mylène Thiery, Eric Coustols *

Aerodynamics and Energetics Modelling Department, Turbulence Modelling and Prediction Unit, ONERA Toulouse, 2 avenue Edouard Belin, 31055 Toulouse Cedex 4, France

Available online 31 March 2006

Abstract

The present study deals with recent numerical results from on-going research conducted at ONERA/DMAE regarding the prediction of transonic flows, for which shock wave/boundary layer interaction is important. When this interaction is strong enough ($M \geqslant 1.3$), shock induced oscillations (SIO) appear at the suction side of the airfoil and lead to the formation of unsteady separated areas. The main issue is then to perform unsteady computations applying appropriate turbulence modelling and relevant boundary conditions with respect to the test case.

Computations were performed with the ONERA **elsA** software and the URANS-type approach, closure relationships being achieved from transport-equation models. Applications are provided for the OAT15A airfoil data base, well documented for unsteady CFD validation (mean and r.m.s. pressure, phase-averaged LDA data, ...).

In this paper, the capabilities of turbulence models are evaluated with two 2D URANS strategies, under free-stream or confined conditions. The latter takes into account the adaptive upper and lower wind-tunnel walls. A complete 3D URANS simulation was then performed to demonstrate the real impact of all lateral wind-tunnel walls on such a flow.

Keywords: Buffet; Shock-induced oscillations; Unsteadiness; RANS; Turbulence modelling; Wind-tunnel-walls effect

1. Introduction

The present study is devoted to the prediction of shock induced oscillations (SIO) over a two-dimensional (2D) rigid airfoil by resolving the unsteady Reynolds-averaged Navier–Stokes (URANS) equations.

For transonic aircraft wing applications, such oscillations are mainly caused by shock wave/boundary layer interaction, which is closely linked to large separated regions. The response of the wing structure to these aerodynamic instabilities (buffet) corresponds to the well-known buffeting phenomenon. These aerodynamic excitations are mainly attributed to pressure fluctuations growing in generated separated areas (e.g. shock footprint, trailing edge, ...). Several studies were devoted to the understanding as well as the control of SIO (Ekaterinaris and Menter, 1994; Gillan et al., 1997; Lee, 2001; Caruana et al., 2003). Although buffeting is not dangerous or destructive for civil aircraft, it mainly affects the aircraft manoeuvrability and consequently the flight envelop. Thus, flow instabilities need to be clearly identified. The present numerical study deals only with aerodynamic issues, even though fluid–structure coupling should be addressed when considering real three-dimensional aircraft wings.

The periodic motion of the shock occurred at a single low frequency (dimensionless frequency $\ll 1$) depending mainly on the airfoil and test section geometries. The turbulence induced next to the wall and in the separated regions is governed by a wide range of high frequencies. The frequency gap between the turbulence and the buffet allows to use the URANS-type approach, the mean flow being resolved from the unsteady RANS solution and the turbulence being modelled.

* Corresponding author. Tel.: +33 5 62252815; fax: +33 5 62 252583.
E-mail address: Eric.Coustols@onera.fr (E. Coustols).

0142-727X/$ - see front matter © 2006 Elsevier Inc. All rights reserved.
doi:10.1016/j.ijheatfluidflow.2006.02.013

Experiments were recently conducted in the transonic wind-tunnel of the ONERA Centre of Chalais Meudon aiming to generate a consistent data base for unsteady CFD validation.

The objectives of the present numerical investigation have been (i) to determine the ability of turbulence models to reproduce unsteady separated flows and (ii) to run computations under conditions as close as possible to the test case, by taking into account the wind-tunnel walls.

2. Test case – OAT15A airfoil

Experiments were rather recently performed in the transonic S3 wind-tunnel of ONERA Centre of Chalais Meudon in the framework of SIO scrutinization (Jacquin et al., 2005). A 2D airfoil (OAT15A cross-section, chord length $c = 230$ mm, relative thickness $t/c = 12.5\%$, blunt trailing edge $e/c = 0.5\%$) was mounted in the test section (0.8×0.76 m^2). The experimental set-up was defined with the aim of providing a two-dimensional flow to the best possible degree compared to previous experiments conducted with such an airfoil in other wind tunnels (Caruana et al., 2003); the aspect ratio of 3.5 was chosen to minimize the 3D effects without fully avoiding them, yet. The upper and lower wind-tunnel walls are adaptive, i.e. flexible instead of being slotted. From the measured wall pressure distributions, the resolution of the linearized Euler equations outside of the test section allows to determine the shape of the walls so that they correspond to flow streamlines. Next, the displacement induced by the presence of the boundary layers is taken into account to adapt the shape of the upper and lower wind-tunnel walls. It has to be pointed out that this technique only allows to adapt the walls to the time-averaged flow.

Tests were carried out at the following aerodynamic conditions: Reynolds number based on the chord length $Re_c = 3 \times 10^6$, free-stream Mach number $M_\infty = 0.73$, stagnation temperature $T_{i\infty} = 300$ K and angles of attack (α) varying from 1.36° to 3.9°. The transition was tripped at $x/c = 7\%$ on both sides of the airfoil using a carborundum band (average height 0.095 mm). The experimental buffet onset appeared at $\alpha = 3.25°$, and the greatest collection of unsteady data was obtained at 3.5°, where the shock moved over about $0.2c$ at a dimensionless frequency of 0.066. Several types of measurements are available for CFD validation purpose: Schlieren type visualisations, time-averaged (static pressure taps and Reynolds-averaged LDA), fluctuating (Kulite transducers) and phase-averaged data (LDA measurements coupled with a conditional analysis).

3. Numerical tools

3.1. Solver and numerical methods

Computations were performed with the ONERA **elsA** software, solving the three-dimensional compressible Reynolds-averaged Navier–Stokes equations for multi-block structured grids, using finite-volume method with cell-centred discretization (Cambier and Gazaix, 2002). The fluxes are computed with two second-order-accurate schemes; the Jameson scheme is used for the mean flow fluxes computation with artificial dissipation terms while the Roe scheme is applied to the turbulent transport equations with an anisotropic correction.

The implicit time integration is performed with the dual-time stepping method which combines (i) a physical time-step, linked to the frequency range of the phenomenon under investigation and (ii) a fictitious dual-time-step, related to a steady process to increase convergence between each physical time-step. The implicit stage is provided by an approached linearization method with a LU factorization associated with a relaxation technique.

Several tests were performed to ensure that the time consistency was reached such that 300 physical time-steps per cycle were imposed to capture unsteadiness (Thiery, 2005). About 10 cycles were necessary to obtain self-sustained SIO while five extra cycles were used to control the periodicity.

3.2. Turbulence modelling

The turbulence closure relies upon the Boussinesq assumption; the eddy viscosity μ_t is then expressed using the turbulent scales (length and velocity) obtained by solving transport equations. Following on previous validations carried out for separated flows (Furlano et al., 2001; Coustols et al., 2003), four models were chosen:

- The one-equation transport model from Spalart and Allmaras (1994), referred to as [SA]. The model was built up empirically to reproduce flows of increasing complexity.
- The two-equation transport model k–ω/k–ε from Menter (1994) in the BaSeLine version, referred to as [BSL]. Menter retained the reliable form while eliminated the free-stream dependency of the k–ω type models.
- The two-equation transport model k–ω/k–ε from Menter (1994) with the shear-stress transport correction, referred to as [SST]. The model is derived from the [BSL] model. The correction applied on the definition of μ_t is based on the Bradshaw's assumption that the principal shear-stress is proportional to the turbulent kinetic energy. Improvements would be brought for adverse pressure gradients boundary layers.
- The two-equation transport model k–kL from Daris and Bézard (2002), referred to as [KKL]. The model is based on a generic form of the transport equations for the turbulent scales and the constants of the model are analytically derived to respect some basic physical features, following Catris and Aupoix (2000), opposite to existing models.

The [SA] and [SST] models have been recommended by NASA Langley for evaluating transonic flows over differ-

ent test cases (Marvin and Huang, 1996), while the [KKL] model has been rather recently developed at ONERA and successfully applied for adverse pressure gradients boundary layers and dynamic stall (Bézard and Daris, 2005). The [BSL] model will provide a reference for the evaluation of the [SST] model.

3.3. Two 2D approaches and one 3D approach

3.3.1. Computational conditions

Earlier studies from Furlano et al. (2001) and Garbaruk et al. (2003) demonstrated the importance of taking into account the wind-tunnel walls for transonic flows. The OAT15A aspect ratio being relatively high, only the upper and lower walls were first considered in a 2D approach (Thiery and Coustols, 2005b).

Two different approaches have been then applied for 2D unsteady computations:

- The "standard" approach, referred to as the "2D inf." approach, whose numerical domain extends over $50c$ to reproduce free-stream conditions. The mesh is composed of about 75,000 grid points, the first cell height $y^+_{1^{st}\text{cell}}$ being about 0.2 (Fig. 1a).
- The "new" approach, referred to as the "2D conf." approach, where the upper and lower wind-tunnel walls are taken into account, treated as viscous walls ($y^+_{1^{st}\text{cell}} \sim 0.4$). The mesh extent was adjusted to reproduce the measured boundary layer thickness at the entrance of the test section. The mesh extended then from $6.5c$ upstream to $4.5c$ downstream of the airfoil and is composed of about 110,000 grid points (Fig. 1b).

Secondly, in order to perform unsteady computations closer to testing conditions, all wind-tunnel walls were considered within a 3D approach. The computational domain was generated from the "2D conf." mesh, some grid points being saved in the middle of the test section. The span-wise characteristics were deduced from previous studies (Furlano et al., 2001) and validated with a steady mesh convergence (Thiery, 2005). A half wind-tunnel was discretized with about 4,000,000 grid points, the side-wall being treated as viscous ($z^+_{1^{st}\text{cell}} \sim 1$).

3.3.2. Aerodynamic conditions

Weak inviscid/viscous coupling computations (ISES-DRELA code) performed at a steady state ($\alpha = 2.5°$) concluded that corrections on M_∞ and α were not necessary for undertaking Navier–Stokes computations under free-stream conditions. The result was assumed to be true for higher α and the boundary conditions for the "2D inf." approach were directly deduced from experimental values of α, Mach and Reynolds numbers.

For the confined 2D and 3D meshes, the experimental total quantities were imposed at the entrance section, while the static pressure was fixed at the exit section to respect

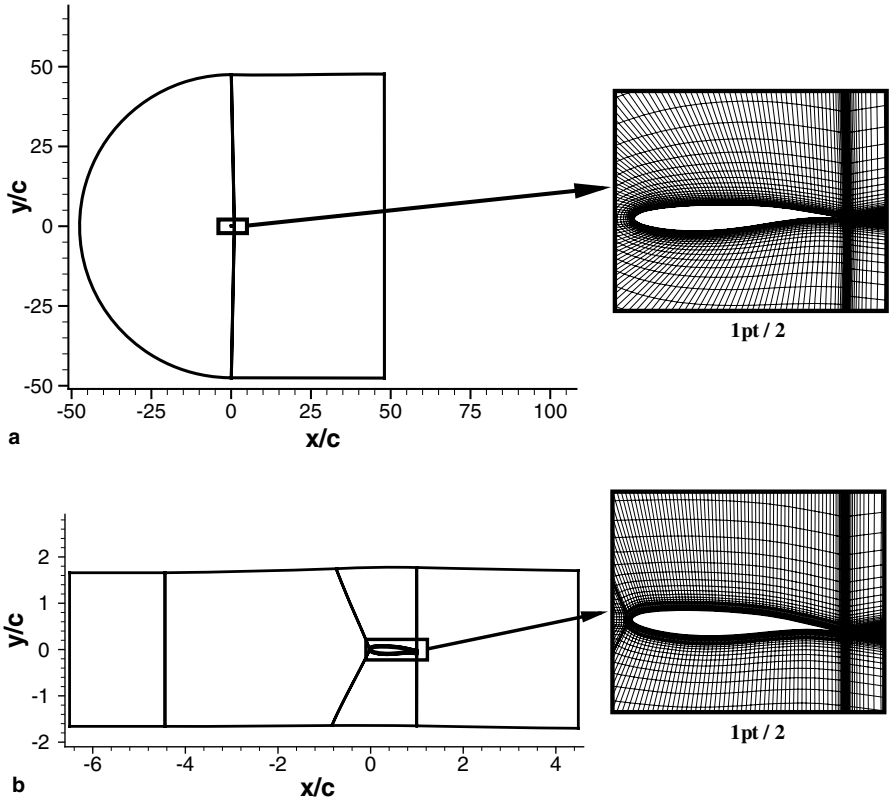

Fig. 1. Sketch of computational domain around the OAT15A airfoil (a: "2D inf." approach, b: "2D conf." approach).

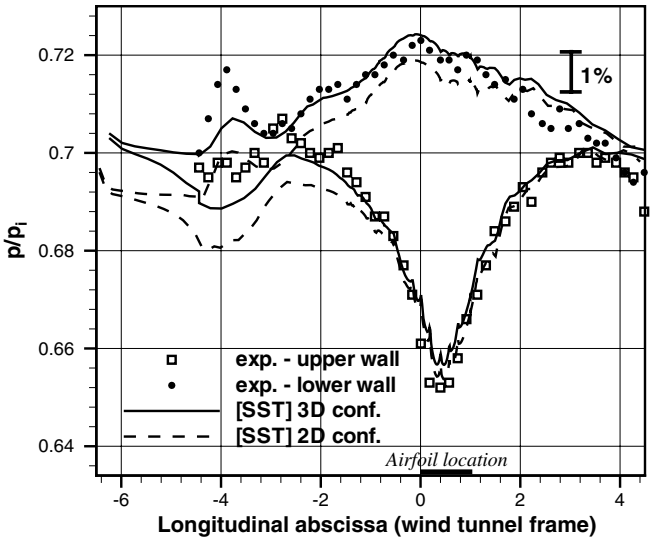

Fig. 2. Time-averaged pressure distributions on the upper and lower wind-tunnel walls for the "2D conf." and "3D conf." approaches – OAT15A airfoil – $M_\infty = 0.73$, $Re_c = 3 \times 10^6$, $\alpha = 3.5°$.

the experimental Mach number. These conditions were validated with time-averaged pressure on the upper and lower walls, illustrated with the [SST] model (Fig. 2).

The evolution along the test section is well reproduced with the "3D conf." approach, while a discrepancy is observed with the "2D conf." approach near the entrance section. For the latter, a compromise has to be found since the computation tends to simulate a 3D mass flow with a 2D-type numerical domain.

4. 2D unsteady results

4.1. Lift evolution versus time

The first step in the turbulence model validation was to check the appearance of self-sustained oscillations: lift evolution versus time is presented in Fig. 3 for the four above-cited models and the two 2D numerical approaches.

Results with the "2D inf." approach (Fig. 3a) highlight a steady behaviour for the [BSL] and [SA] models while the [KKL] and [SST] models develop lift oscillations. Steady solution recorded with the [SA] model under free-stream conditions is not consistent with previous studies on SIO or separated flows (Coustols et al., 2003). Investigations on the grid refinement, the mesh topology or the over-thickening of the boundary layer at the tripping location were carried out with that model but did not bring any improvement. Only an increase of more than one degree of incidence allowed to develop SIO with the "2D inf." approach (Thiery and Coustols, 2005a).

By taking into account the upper and lower wind-tunnel walls (Fig. 3b), the [SA] model can develop unsteadiness while the state of the computed flow is unchanged with the [BSL], [KKL] and [SST] models. The lift oscillation amplitudes of the [KKL] (respectively [SST]) model are increased by a factor of 2 (respectively 2.5) compared to results for the "2D inf." approach. However, the time-averaged lift coefficient is constant whatever the approach.

For a given approach, either "2D inf." or "2D conf.", comparisons between turbulence models demonstrate large discrepancies on the time-averaged lift coefficient; this is closely linked to the difficulty to correctly predict the shock location since the pressure gradient is nearly null upstream of the shock. For the "2D inf." approach (Fig. 3a), the lift amplitude of the [KKL] model is two times larger than the [SST] model one, while accounting for the test section walls widely reduces the gap between the two models. For the "2D conf." approach (Fig. 3b), the [KKL] and [SST] models predict oscillations about two times larger than those of the [SA] model. The SST correction brings strong improvement to the [BSL] model behaviour, allowing to compute unsteady flow, whatever the approach.

Lastly, the dimensionless computed SIO frequency is slightly dependent upon the turbulence model (~0.068–0.075, for 71–78 Hz). When the wind-tunnel walls are modelled, a decrease of 3 Hz is observed whatever the model, predictions being closer to the experimental value (0.066). These results demonstrate that the frequency is not a selective parameter for turbulence models validation; it is consistent with the buffet modelling proposed by Lee (2001) who argued that the frequency is mainly governed by the airfoil and test section geometries.

The fact that a constant static pressure is prescribed at the exit section, imposing then perturbations to be damped, raises the question of the dependency of the SIO frequency upon the domain extent. That point was addressed in Thiery and Coustols, 2005c by generating a new grid, the exit section being shifted from 4.5 to 8.5c downwards: unsteady results with the [SA] model were unchanged.

4.2. Pressure distributions

4.2.1. Time-averaged pressure distributions

The time-averaged pressure distributions help to evaluate turbulence models on the prediction of time-averaged load (Fig. 4a and b).

The experimental distribution is quite usual for such an airfoil. The suction side is composed of three main parts, the supersonic plateau ($0.05 \leqslant x/c \leqslant 0.35$), the spread compression due to the unsteady shock wave ($0.35 \leqslant x/c \leqslant 0.55$) and the recompression zone ($x/c \geqslant 0.55$). The pressure side is characterised by the rear load caused by the specific airfoil curvature.

The pressure side and the supersonic plateau are quite well predicted whatever the model or the approach. For the "2D conf." approach, it confirms that the aerodynamic conditions for the airfoil were well adjusted and the adaptation of the wind-tunnel walls was well managed for the time-averaged flow.

Main discrepancies are observed on the location of the shock wave and on the width of its effect on pressure distri-

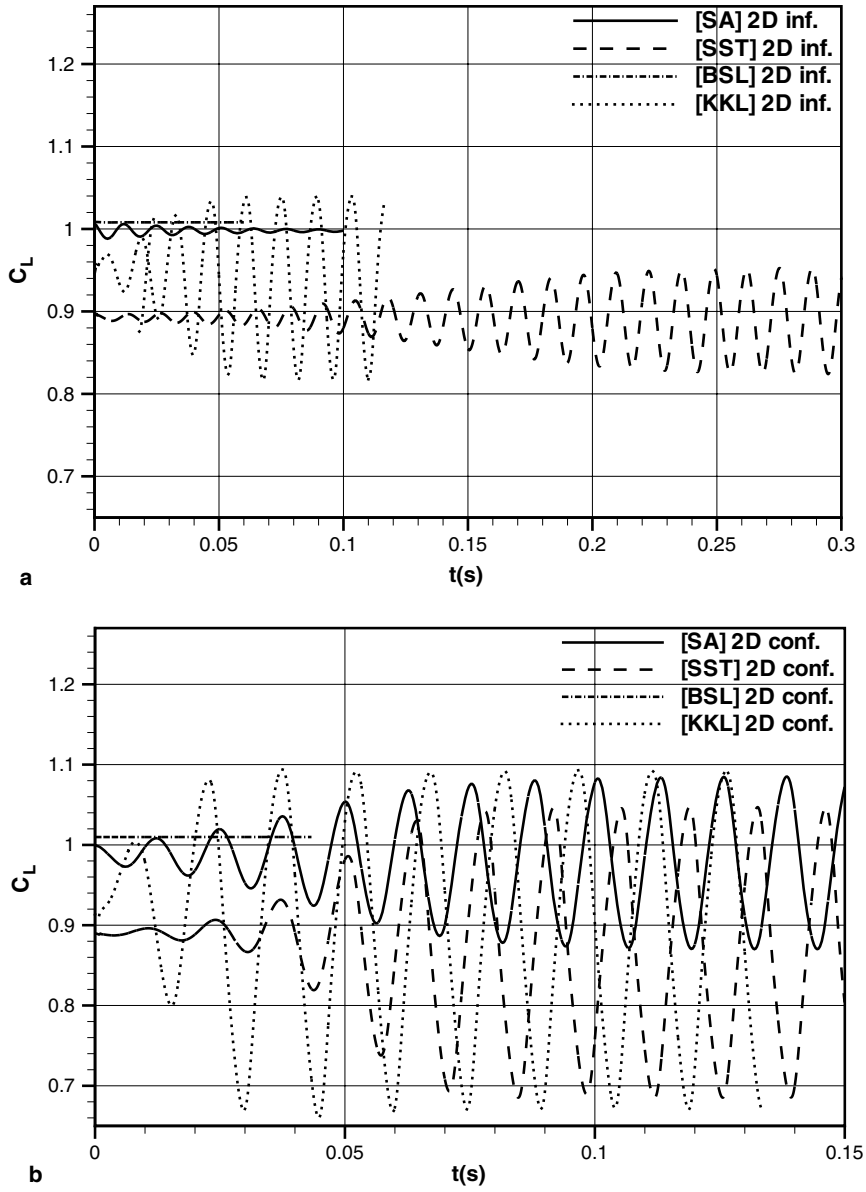

Fig. 3. Lift evolution versus time (a: "2D inf." approach, b: "2D conf." approach) OAT15A airfoil – $M_\infty = 0.73$, $Re_c = 3 \times 10^6$, $\alpha = 3.5°$.

bution. These predictions depend on the unsteady content of the numerical solution and they will be then commented with r.m.s. pressure distributions.

The recompression is quite badly reproduced under free-stream conditions while all turbulence models fit the experimental evolution in the rear part with the confined approach.

4.2.2. Unsteady r.m.s. pressure distributions

The unsteady r.m.s. pressure distributions along the airfoil are discussed to evaluate the levels of unsteadiness provided by the computations and to compare them to the measured ones (Fig. 5a and b). Typically, three main levels can be distinguished; (i) small levels ($\sim 0.02 q_0$) on the pressure side and on the first 30% of the suction side, (ii) medium levels ($\sim 0.1 q_0$) in the unsteady separated area downstream the shock ($x/c \geqslant 0.6$) and, (iii) large levels ($\sim 0.3 q_0$) in the vicinity of the shock location ($0.4 \leqslant x/c \leqslant 0.6$).

Considering the "2D inf." approach (Fig. 5a) and applying the [SST] model, numerical values are in very good agreement with the experimental ones though the levels are slightly under-estimated all over the airfoil. The location of the time-averaged shock, which corresponds approximately to the maximum of fluctuations, is rather well predicted. The [KKL] model predictions demonstrate stronger fluctuations and a wider range of SIO than the [SST] model do. Moreover, the maximum of fluctuation is $0.08c$ downstream of the experimental one.

Concerning the "2D conf." approach (Fig. 5b), fluctuations increase for the [SST] and [KKL] models as pointed out with the time-evolution of the lift coefficient. The results are degraded especially on the pressure side and upstream of the shock. The [SA] model is in better

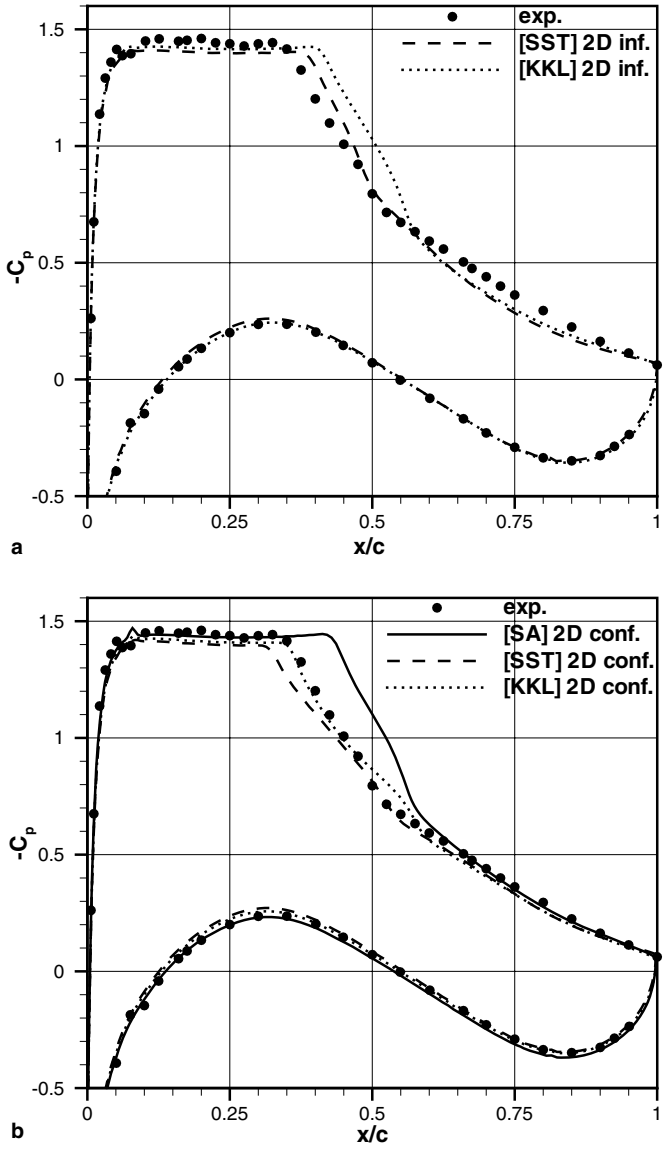

Fig. 4. Time-averaged pressure distributions (a: "2D inf." approach, b: "2D conf." approach) – OAT15A airfoil – $M_\infty = 0.73$, $Re_c = 3 \times 10^6$, $\alpha = 3.5°$.

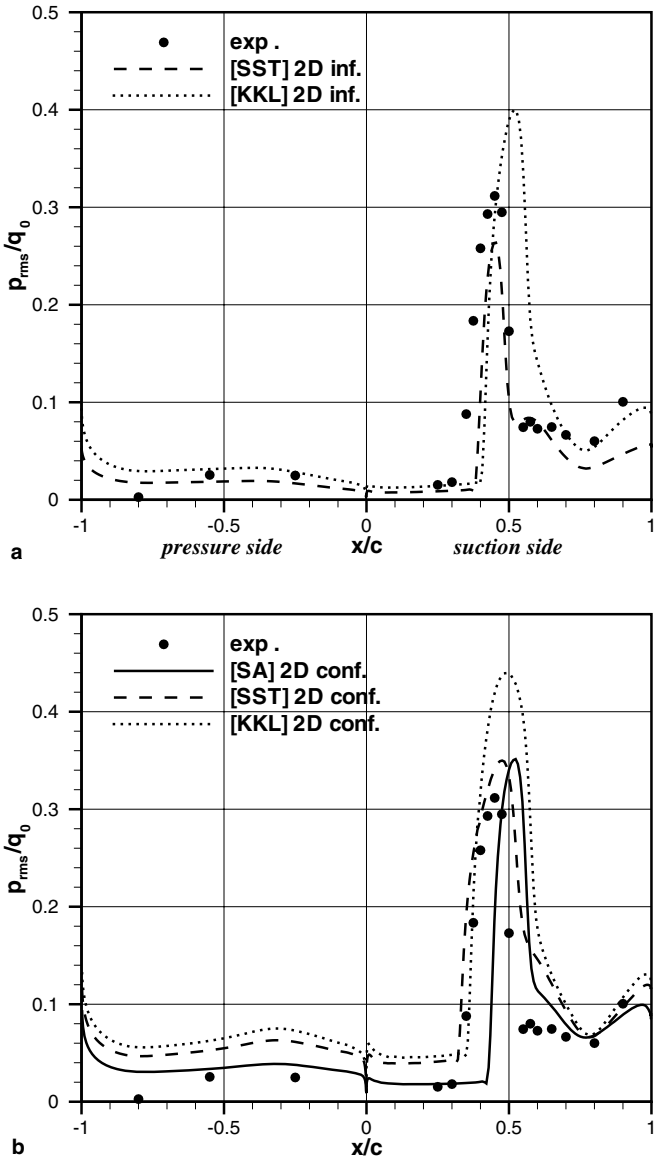

Fig. 5. Unsteady r.m.s. pressure distributions (a: "2D inf." approach, b: "2D conf." approach) – OAT15A airfoil – $M_\infty = 0.73$, $Re_c = 3 \times 10^6$, $\alpha = 3.5°$.

agreement with the experiments but the location of the time-averaged shock is $0.08c$ downstream of the experimental one. Lastly, the predictions of all models gather for $0.6 \leqslant x/c \leqslant 1$ and reproduce quite well the experimental evolution, particularly the fluctuation increase next to the trailing edge. This result might indicate that the unsteady separated area is mainly governed by the shock instability, enhanced by the modelling of the wind-tunnel walls.

The time-averaged pressure distributions on the upper and lower wind-tunnel walls are not really affected by turbulence modelling. For the r.m.s. pressure distributions (Fig. 6), the results obtained with the three turbulence models have quite similar evolutions along the upper and lower wind-tunnel walls, levels being ordered in the same way as on the airfoil (Fig. 5a and b). In the upstream part of the test section ($l/c \leqslant -2$, where l denotes the longitudinal abscissa in the wind tunnel frame), fluctuations are nearly constant ($\sim 0.02 q_0$) and equivalent to the levels computed on the pressure side of the airfoil. Next to the airfoil location ($0 \leqslant l/c \leqslant 1$), the r.m.s. pressure distributions reach a maximum equal to about 15% of the maximum of fluctuations reached on the airfoil. For $l/c \geqslant 1$, the levels decrease to zero since the boundary condition at the exit section imposes a constant static pressure. Then, the fluctuations on the upper and lower wind-tunnel walls exist and are not negligible with respect to the airfoil ones. Indeed, the adaptation of the walls was managed for the time-averaged flow.

4.3. Phase-averaged boundary layer profiles

The SIO period was discretized in 20 phases and for five of them, the numerical unsteady profiles are compared to

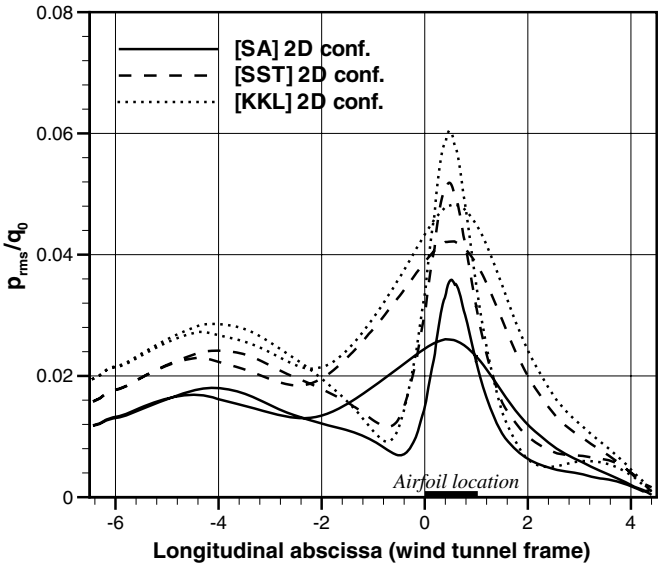

Fig. 6. Unsteady r.m.s. pressure distributions on the upper and lower wind-tunnel walls for the "2D conf." approach – OAT15A airfoil – $M_\infty = 0.73$, $Re_c = 3 \times 10^6$, $\alpha = 3.5°$.

the experimental ones (Fig. 7). The velocity profiles were extracted downstream of the shock ($x/c = 0.6$) where the boundary layer is periodically attached (seven phases from 4T to 11T/20) and partially separated (eleven phases from 12T to 3T/20).

For the "2D inf." approach (Fig. 7a), the experimental time-evolution of the boundary layer profile is well reproduced when applying the [SST] model. Nonetheless, the intensity of the back-flow seems to be under-estimated. The [KKL] model prediction is not far from experiments but demonstrates a delay to develop the separated area, which can induce a large error on the boundary layer thickness (e.g. about 35% at phase 13T/20). The problem might be linked to the poor prediction of the shock location (maximum of computed fluctuations located $0.08c$ downstream of the experimental one).

The impact of the upper and lower wind-tunnel walls on the boundary layer profiles is very important for the predictions provided by the [SST] and [KKL] models (Fig. 7b). At phase 1T/20, the computed boundary layers are completely attached while the measured one is separated. At phase 17T/20, the thickness of the separated region is widely over-estimated (~30%). The [SA] model result provides the best prediction using the "2D conf." approach, with a delay to develop the separated region at phase 13T/20, yet.

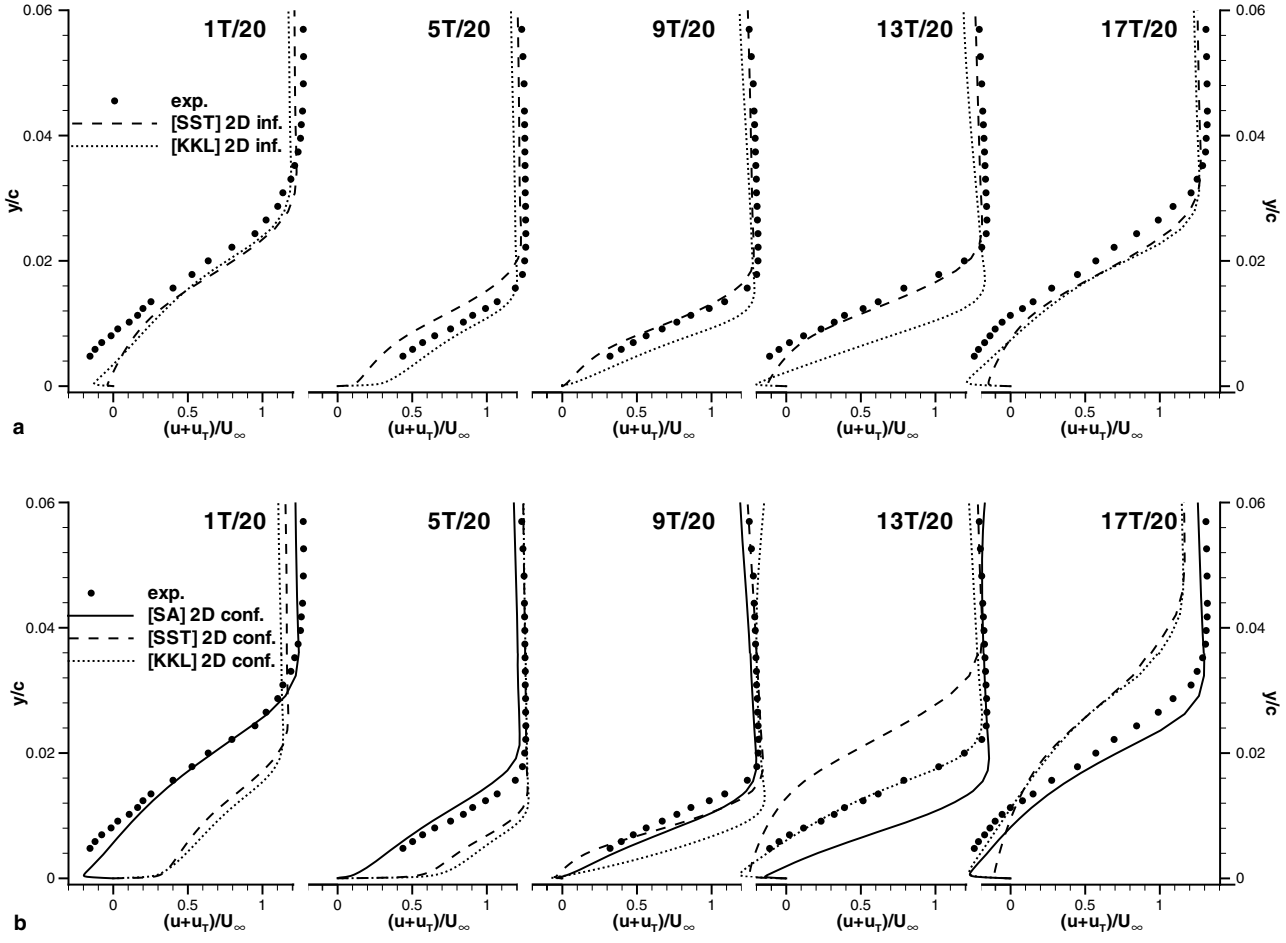

Fig. 7. Unsteady velocity profiles at $x/c = 0.6$ for five phases in the SIO period sliced into 20 phases (a: "2D inf." approach, b: "2D conf." approach) – OAT15A airfoil – $M_\infty = 0.73$, $Re_c = 3 \times 10^6$, $\alpha = 3.5°$.

These results are really encouraging since all models are based on the Boussinesq hypothesis (local closure), which does not figure on enough "history" effect and does not correctly simulate the momentum transfer in the separated areas. That might be another evidence that the separation downstream of the shock is mainly governed by the shock instability, and not by the turbulence modelling.

4.4. Concluding remarks on "2D conf." approach

The modelling of the upper and lower wind-tunnel walls increase the unsteady content of the 2D numerical solution. Indeed, the walls have a time-averaged deformation, impose the instantaneous flow streamlines to be constant in their vicinity and generate a blocking effect on the unsteady flow.

Moreover, the wind-tunnel side walls complete the experimental confinement and one can wonder their influence on the unsteadiness measured in the centreline. The side walls are then modelled within a 3D computation to evaluate their role on the SIO development.

5. 3D unsteady results

In this section, the effect of the wind-tunnel side walls will be addressed using only the [SST] model which provided satisfactory unsteady solutions with respect to the two 2D approaches.

5.1. Lift evolution and pressure distribution

First, the time-evolution of the lift coefficient is provided in the box at the top-left in Fig. 8, with a comparison to the two 2D approaches. The 3D lift amplitude is quite similar to the one computed with the "2D inf." approach, the "2D conf." oscillation being three times larger.

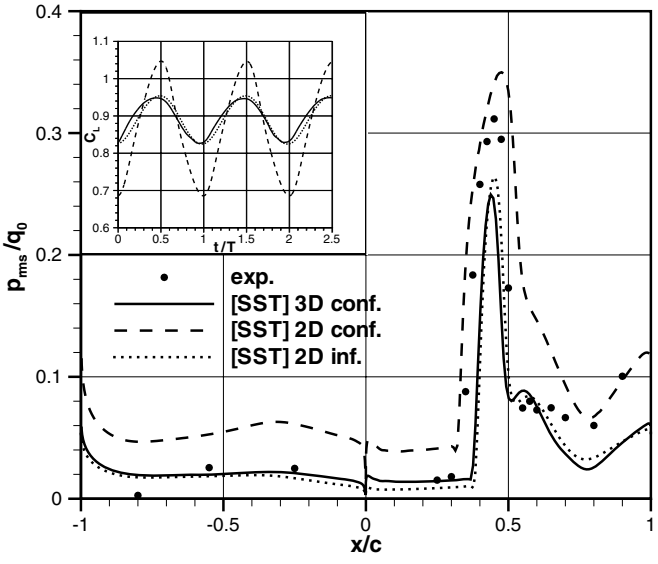

Fig. 8. Lift evolution versus time and r.m.s. pressure distributions along the airfoil obtained with the [SST] model for the "2D inf.", "2D conf." and "3D conf." approaches – OAT15A airfoil – $M_\infty = 0.73$, $Re_c = 3 \times 10^6$, $\alpha = 3.5°$.

Along the airfoil, the r.m.s. pressure distributions computed with the "3D conf." approach at the wind-tunnel centreline are in agreement with the experimental levels on the pressure side and the first 30% of suction side (Fig. 8). However, the SIO extent and r.m.s. maximum are slightly under-estimated, as well as the fluctuations in separated zone ($x/c \geqslant 0.6$).

The 3D unsteady content is similar to the one obtained with the "2D inf." approach. The fluctuation increase induced by the 2D blocking effect is then totally balanced by the decrease generated by the modelling of the wind-tunnel side-wall. The same trend was observed on a swept wing (OAT15A airfoil cross-section) by Brunet (2005); the computation being performed with lateral walls, but without upper and lower walls.

The r.m.s. pressure distributions along the upper and lower walls of the test section are weaker than when running the 2D confined approach. The level is then similar to that recorded on the pressure side of the airfoil (Thiery, 2005).

5.2. Phase-averaged boundary layer profiles

Phase-averaged boundary profiles are provided in Fig. 9. The 3D simulation estimates rather well the shear layer for phases 5T/20 and 9T/20. The back-flow is under-estimated at the following instants in the SIO period. For phase 1T/20, the boundary layer reattachment is advanced with respect to the experimental time-evolution.

The "3D conf." approach prediction is again close to the "2D inf." one but some discrepancies appear, mainly noticeable as phase-lags (5T/20, 13T/20 and 1T/20). The 2D results under free-stream conditions are in better agreement with experimental values than the 3D ones. Nonetheless, the comparison might be skewed by the turbulent relationship, which is a first-order closure and can induce some phase-lags on shear stresses for quick alteration of the velocity gradients.

5.3. 3D flow topology evolution versus time

Instantaneous friction-lines and pressure coefficient are represented on the airfoil suction side and the wind-tunnel side-wall (Fig. 10). The 3D flow topology is composed of typical flow patterns: the dividing line at the shock footprint, the shock induced separation and some complex windings, associated to the corner separation and generated by the interaction between the airfoil and the side-wall.

At the phase 1T/20, the shock wave is located at its more upstream position and induces a separation at its footprint. The flow topology next to the centreline is nearly 2D but is quite complex in the vicinity of the side-wall. When the shock moves downwards, the windings in the corner separation are ejected in the wake so that the flow pattern is simpler.

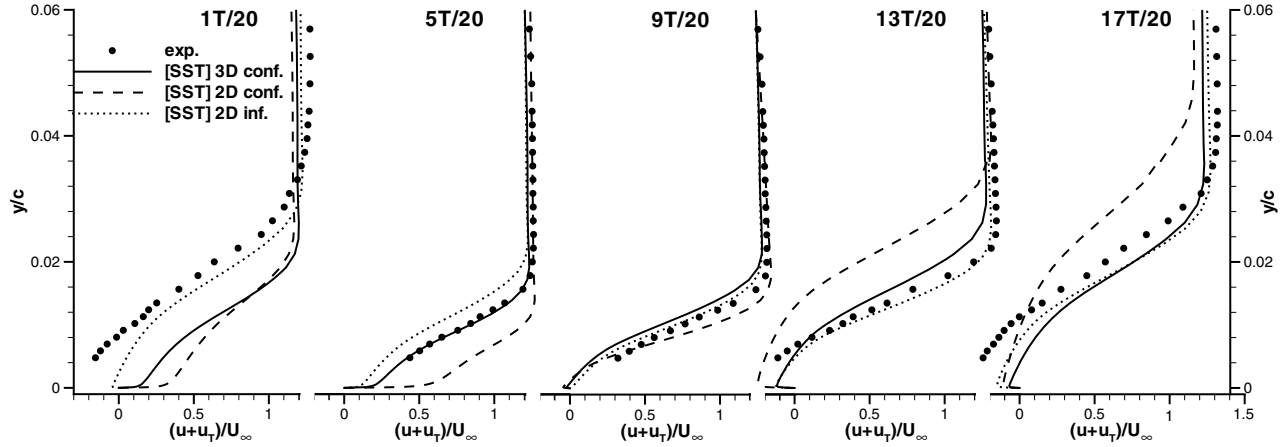

Fig. 9. Unsteady velocity profiles at $x/c = 0.6$ for five phases in the SIO period sliced into 20 phases obtained with the [SST] model and the "2D inf.", "2D conf." and "3D conf." approaches – OAT15A airfoil – $M_\infty = 0.73$, $Re_c = 3 \times 10^6$, $\alpha = 3.5°$.

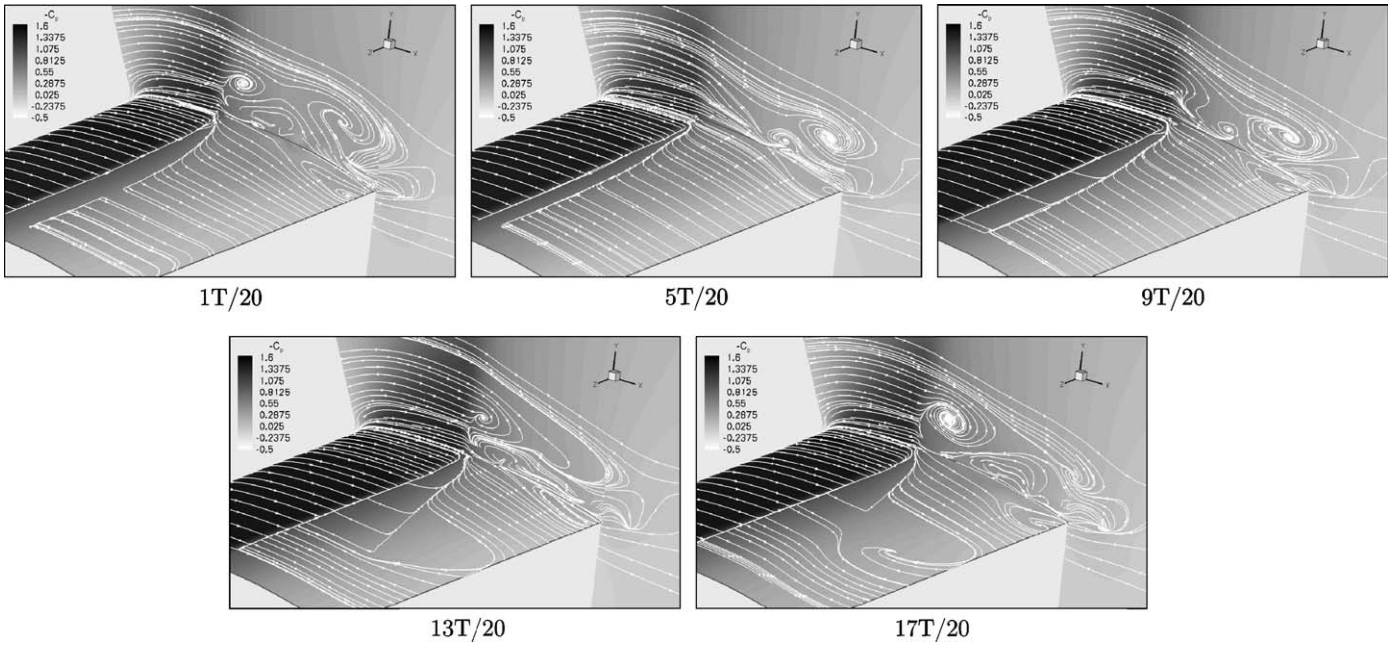

Fig. 10. 3D friction-lines and pressure coefficient for five phases in the SIO period sliced into 20 phases obtained with the [SST] model and the "3D conf." approach – OAT15A airfoil – $M_\infty = 0.73$, $Re_c = 3 \times 10^6$, $\alpha = 3.5°$.

At the phase 9T/20, the shock wave is close to its more downstream location and the windings in the vicinity of the side-wall are more complex and extended. That trend is reinforced when the shock moves upwards and a mid-span roll is generated.

The flow in the vicinity of the wind-tunnel centreline is then disturbed for the extreme shock locations (1T/20 and 10T/20) but remains 2D for others instants in the SIO period.

6. Concluding remarks

Presented results dealt with unsteady computations of shock induced oscillations (SIO). A turbulence model validation has been performed and applied to the 2D rigid OAT15A airfoil test case with two 2D approaches: (i) the "2D inf." approach under free-stream conditions and (ii) the "2D conf." approach in which the upper and lower walls were taken into account.

Four turbulence models were evaluated: the [SA], [BSL], [SST] and [KKL] models. Unsteady results obtained with the [SST] and [KKL] models with the "2D inf." approach highlighted their ability to easily develop separated areas while the [SA] model needed to be triggered by the modelling of the upper and lower walls of the test section to predict SIO. The wind-tunnel walls modelling had no effect on the steady results obtained with the [BSL] model, though the [SST] and [KKL] predictions were completely

destabilized and moved away from experiments. The SST correction improved the behaviour of the [BSL] model with respect to the prediction of the separated regions. For 2D simulation, it looked like the best agreement with the experimental observations was obtained with the [SST] model.

Moreover, the [SST] model was the only one to develop unsteadiness with the "3D conf." approach, resolving remarkably well the blocking effect generated by the corner separation.

The fluctuations in the separation downstream of the shock seemed to be mainly governed by the shock instability, not by the turbulence modelling. The latter allowed unsteadiness to develop and influenced the amplitude of the shock motion. The frequency appeared to be mainly linked to the inviscid flow.

The major influence of the modelling of the upper and lower wind-tunnel walls was to increase the fluctuation levels along the airfoil. Nonetheless, this effect was completely balanced when taking into account the side walls. The pressure fluctuations on the upper and lower walls of the wind-tunnel are thus small with respect to the total dynamic pressure ($\sim$2%). Therefore, the modelling of wind-tunnel walls should not be necessary to objectively evaluate the capabilities of turbulence models to capture SIO on our selected test case.

Acknowledgements

The authors gratefully acknowledge the Service des Programmes Aéronautiques which granted research reported in the paper. The authors would like to warmly thank the editor, who encouraged them to enlarge consequently the first reviewed version of the paper in order to fulfil reviewers' comments. The valuable comments by the two reviewers are thankfully acknowledged.

References

Bézard, H., Daris, T., 2005. Calibrating the length scale equation with an explicit algebraic Reynolds stress constitutive relation. In: Rodi, W. (Ed.), Proceedings, Engineering Turbulence Modelling and Experiments, 6. Elsevier Ltd., pp. 77–86.

Brunet, V., 2005. Simulation numérique par l'approche URANS des instabilités aéro-dynamiques en régime transsonique, ONERA Technical Report, DAAP 4/08377.

Cambier, L., Gazaix, M., 2002. **elsA**: an efficient object-oriented solution to CFD complexity. In: Proceedings, 40th AIAA Aerospace Sciences Meeting & Exhibit, Reno, Nevada, USA, AIAA Paper 2002-0108.

Caruana, D., Mignosi, A., Robitaillé, C., Corrège, M., 2003. Separated flow and buffeting control. Flow, Turbulence and Combustion 71 (1–4), 221–245.

Catris, S., Aupoix, B., 2000. Towards a calibration of the length-scale equation. International Journal of Heat and Fluid Flow 21 (5), 606–613.

Coustols, E., Schaeffer, N., Thiery, M., Cordeiro Fernandes, P., 2003. Unsteady Reynolds-averaged Navier–Stokes computations of shock induced oscillations over two-dimensional rigid airfoils. In: Proceedings, 3rd International Symposium of Turbulence and Shear Flow Phenomena, Sendaï, Japan, June 25–27, vol. 1, pp. 57–62.

Daris, T., Bézard, H., 2002. Four-equations models for Reynolds stress and turbulent heat flux predictions. In: Proceedings, 12th International Heat Transfer Conference, Grenoble, France, August 18–23.

Ekaterinaris, J.A., Menter, F.R., 1994. Computation of separated and unsteady flows with one- and two-equation turbulence models. AIAA Journal 32, 23–59.

Furlano, F., Coustols, E., Rouzaud, O., Plot, S., 2001. Steady and unsteady computations of flows close to airfoil buffeting: validation of turbulence models. In: Proceedings, 2nd International Symposium on Turbulence and Shear Flow Phenomena, Stockholm, Sweden, June 27–29, vol. 1, pp. 211–216.

Garbaruk, A., Shur, M., Strelets, M., Spalart, P.R., 2003. Numerical study of wind-tunnel walls effects on transonic airfoil flow. AIAA Journal 41 (6), 1046–1054.

Gillan, M.A., Mitchell, R.D., Raghunathan, S.R., Cole, J.S., 1997. Prediction and control of periodic flows. In: Proceedings, 35th AIAA Aerospace Sciences Meeting & Exhibit, Reno, Nevada, USA, AIAA Paper 1997-0832.

Jacquin, L., Molton, P., Deck, S., Maury, B., Soulevant, D., 2005. Experimental study of the 2D oscillation on a transonic wing. In: Proceedings, 35th AIAA Fluid Dynamics Conference, Toronto, Canada, June, AIAA Paper 2005-4902.

Lee, B.H.K., 2001. Self-sustained shock oscillations on airfoils at transonic speeds. Progress in Aerospace Sciences 37, 147–196.

Marvin, J.G., Huang, G.P., 1996. Turbulence modeling. Progress and future outlook. In: Proceedings, 5th International Conference on Numerical Methods in Fluid Dynamics, Monterey, CA, USA, June 24–28.

Menter, F.R., 1994. Two-equation eddy-viscosity turbulence models for engineering applications. AIAA Journal 32 (8), 1598–1605.

Spalart, P.R., Allmaras, S.R., 1994. A one-equation turbulence model for aerodynamic flows. La Recherche Aérospatiale 1, 5–21.

Thiery, M., 2005. Modélisation numérique du tremblement sur profil d'aile supercritique. Ph.D. Thesis SUPAERO Toulouse, 1st December 2005.

Thiery, M., Coustols, E., 2005a. URANS Computations of Shock Induced Oscillations Over 2D Rigid Airfoil: Influence of Test Section Geometry. In: Proceedings, 6th ERCOFTAC International Symposium on Engineering Turbulence Modelling and Measurements, Sardinia, Italy, May 23–25, pp. 637–646.

Thiery, M., Coustols, E., 2005b. Numerical prediction of shock induced oscillations over 2D rigid airfoil: influence of turbulence modelling and wind tunnel walls. In: Proceedings, 4th International Symposium of Turbulence and Shear Flow Phenomena, Williamsburg, Virginia, May 23–25, vol. 3, pp. 947–952.

Thiery, M., Coustols, E., 2005c. URANS computations of shock-induced oscillations over 2D rigid airfoils: influence of test section geometry. Flow, Turbulence and Combustion 74 (4), 2005.